

Document downloaded from:

<http://hdl.handle.net/10251/64103>

This paper must be cited as:

Leus, K.; Concepción Heydorn, P.; Vandichel, M.; Meledina, M.; Grrirane, A.; Esquivel, D.; Turner, S.... (2015). Au@UiO-66: a base free oxidation catalyst. RSC Advances. 5(29):22334-22342. doi:10.1039/C4RA16800C.



The final publication is available at

Copyright Royal Society of Chemistry

Additional Information

Au@UiO-66: a base free oxidation catalyst

Karen Leus¹, Patricia Concepcion², Maria Meledina³, Abdessamad Gurrane², Dolores Esquivel¹, Stuart Turner³, Dirk Poelman⁴, Gustaaf Van Tendeloo³, Hermenegildo García², Pascal Van Der Voort^{1*}

¹ Department of Inorganic and Physical Chemistry, Center for Ordered Materials, Organometallics and Catalysis (COMOC), Ghent University, Krijgslaan 281-S3, 9000 Ghent, Belgium.

² Instituto de Tecnología Química, CSIC-UPV, Universidad Politécnica de Valencia, Av. de los Naranjos s/n, 46022 Valencia (Spain).

³ Electron Microscopy for Materials Science (EMAT), University of Antwerp, Groenenborgerlaan 171, 2020 Antwerp, Belgium.

⁴ Department of Solid State Sciences, Lumilab, Ghent University, Krijgslaan 281- S1, 9000 Ghent, Belgium.

Abstract

We present the *in situ* synthesis of Au nanoparticles within a Zr based Metal Organic Framework, denoted as UiO-66. The resulting Au@UiO-66 materials were characterized by means of N₂ sorption, XRPD, UV-Vis, XRF, XPS and TEM analysis. The results demonstrate that the Au NP are homogeneously distributed along the UiO-66 host matrix using NaBH₄ or H₂ as reducing agents. Additionally, the Au@UiO-66 materials were evaluated as a catalyst in the oxidation of benzyl alcohol and benzyl amine employing O₂ as oxidant. The Au@MOF materials exhibits a very high selectivity towards the keton (up to 100 %). Regenerability and stability tests have been carried out demonstrating that the Au@UiO-66 catalyst can be recycled with a negligible loss of Au species and no loss of crystallinity. Moreover *in situ* IR measurements were carried out.....

Keywords: Metal Organic Framework, oxidation, aerobic, gold, nanoparticles

1. Introduction

Since the breakthrough discovery by Haruta et al. on the use of Au nanoparticles (NP) for the low temperature aerobic oxidation of carbon monoxide many other aerobic oxidation reactions have been reported¹. For instance gold NP have been used to catalyze the selective oxidation of hydrocarbons, sugars, carbonyl compounds, alcohols and in the oxidation of amines to amides². Nevertheless, a severe problem in gold catalysis is their facile sintering and irreversible aggregation. To stabilize the gold NP many different supports have been examined as host material. The most commonly employed support materials are metal-oxides e.g. CeO₂, TiO₂, Al₂O₃³ but also carbon and silica based materials have been extensively investigated as host material⁴

Alternatively, attempts have been made to synthesize NP containing organic frameworks as well. This is another efficient way to stabilize NP. Metal Organic Frameworks (MOFs) are crystalline porous materials constructed from metal ions or metal clusters interconnected by rigid organic linkers. MOFs have been examined for many potential applications, for example in gas sorption and separation, sensing,

luminescence and in catalysis⁵. In the latter field there is an increasing interest towards the embedding of NP in MOFs. Thus far, Pd, Ru, Cu, Pt, Ni, Ag and Au NP have been incorporated in MOFs⁶. All the reported Au@MOF materials were examined for the liquid phase oxidation of benzyl alcohol. However, different reaction conditions were used in the catalytic studies. Firstly, there is a lot of debate on the question if a base is required. Müller et al. showed that if no base was added to the reaction mixture, the Au@MOF-5, Au/ZnO@MOF-5 and Au/TiO₂@MOF-5 catalyst showed no catalytic activity in the oxidation of benzyl alcohol, whereas in the presence of the base K₂CO₃, the oxidation reaction is accelerated by deprotonation of the alcohol⁷. Nonetheless, in the report of Liu et al. concerning Au@MIL-101, the Au@MOF material could efficiently catalyze the oxidation of alcohols under ambient conditions in the absence of a base⁸. The high dispersion of the Au NP and the electron donation effects of the aryl rings to the Au NP within the cages of the MIL-101 support are put forward to be the main reason for the high activity. It is suggested that the support may play a crucial role, either direct or indirect, in the determination of the activity of gold⁹. The influence of the support is also illustrated in the work of Ishida et al. in which large differences in alcohol conversions are observed for the Au@MOF-5, Au@Al-MIL-53, and Au@Cu₃(BTC)₂¹⁰. Also in the work of Esken et al. it was suggested that the Au NP may chemically interact with the functionalities on the organic linker. They observed a remarkable difference in catalytic activity between Au@ZIF-8, which exhibit a good conversion of 81% benzyl alcohol, whereas the Au@ZIF-90 shows a very weak activity (13%). The latter is due to *in situ* oxidation of the aldehyde functions of ZIF-90 by means of the Au NP imbedded in the MOF, making the active Au sites inaccessible for further reaction¹¹. Very recently Zhu et al.¹² reported on the synthesis of Au@UiO-66 which was examined in the oxidation of benzyl alcohol in the presence of O₂ and a base. However, to the best of our knowledge no detailed mechanistic studies were carried out aiming at understanding the influence of the MOF support on the catalytic activity of the Au NP. In this paper we report on the *in situ* synthesis and characterization of Au NP in a zirconium containing MOF, denoted as UiO-66. The resulting Au@UiO-66 material was evaluated in the oxidation of benzyl alcohol and benzyl amine using oxygen as the only oxidant. Additionally regenerability and stability tests were carried out. Finally *in situ* IR measurements were done....

2. Materials and methods

2.1 General procedures

All chemicals were purchased from Sigma Aldrich or TCI Europe and used without further purification. Nitrogen adsorption experiments were carried out at -196 °C using a Belsorp-mini II gas analyzer. Prior to analysis, the samples were dried under vacuum at 120 °C to remove adsorbed water. X-Ray powder diffraction (XRPD) patterns were collected on a ARL X'TRA X-ray diffractometer with Cu K α radiation of 0.15418 nm wavelength and a solid state detector. X-ray Fluorescence (XRF) measurements were performed on a NEX CG from Rigaku using a Mo-X-ray source. UV-Vis measurements were carried out on a Varian Cary 500 dual beam UV-Vis-Near IR spectrophotometer, applying an internal 110 mm BaSO₄-coated integrating sphere. Elemental analyses of the leached species after catalysis were performed by inductively coupled plasma-optical emission spectroscopy (ICP-OES) on a Varian 715-ES. Prior to analysis, the catalytic mixture was evaporated to dryness and redissolved in an H₂SO₄ aqueous solution. Gas chromatography (GC) experiments were conducted on a Varian 3900 apparatus

equipped with an TRB-5MS column (5% phenyl, 95% poly- methylsiloxane, 30 m, 0.25 mm x0.25 μ m, Teknokroma) using He as carrier gas. The reaction products were identified with a GC/MS spectrometer from Agilent equipped with the same column as the GC and operated under the same conditions. XPS spectra were recorded with a SPECS Phoibos HAS 3500 150 MCD. The X-ray source was generated by a Mg anode ($h\nu = 1253.6$ eV) powered at 12 kV and with an emission current of 25 mA. The samples were pressed and introduced into the spectrometer without previous thermal treatment. They were outgassed overnight and analyzed at room temperature. Accurate binding energies (BE) have been determined with respect to the position of the C 1s peak at 284.8 eV. The peaks were decomposed using a least-squares fitting routine (Casa XPS software) with a Gauss/Lorenz ratio of 70/30 and after subtraction of a linear background.

TEM and in situ IR measurements

2.2 Synthesis of UiO-66

The UiO-66 material was synthesized according to the recipe described by Biswas et al.¹³ 0.31mmol of $ZrO_2Cl_2 \cdot 8H_2O$ was mixed together with 0.31mmol of terephthalic acid in 1.2 mL formic acid and 3 mL dimethylacetamide. The resulting mixture was placed for 24 hours at 150 °C, filtered off and washed several times with acetone. The resulting UiO-66*as* was stirred respectively in DMF for 12 hours and in methanol for 24 hours at room temperature to remove unreacted linker. Hereafter the sample was dried under vacuum at 65 °C for 24 hours prior to use.

2.3 Synthesis of Au@UiO-66

The Au@UiO-66 materials were obtained by mixing 0.15 g of UiO-66 with 7 mg of $HAuCl_4$ in 40 mL of MeOH. The resulting mixture was stirred at RT for 6 hours under a nitrogen atmosphere. Hereafter three different methods were examined to reduce the gold. In the first method, $NaBH_4$ was added (10 times excess) and stirred for an additional 1 hour at RT before filtration, the resulting sample is denoted as Au@UiO-66- $NaBH_4$. In a second method, triethylamine (30 times excess) was added as reducing agent to the mixture and stirred for 1 hour at RT. In the following this sample will be referred to as Au@UiO-66-triethylamine. In a third method, the Au@UiO-66 was placed for 2 hours at 200 °C under a H_2 /argon stream, the resulting sample was denoted as Au@UiO-66- H_2 .

2.4 Catalytic setup

In each catalytic test 0.25 mmol of the substrate was loaded in the reactor together with 1mL of toluene (solvent) and 0.10 mmol of dodecane (used as internal standard). 2 mol % (0.005mmol) of the catalyst was added to the reaction mixture before sealing the reactor and placing it under a pressure of 5 bar O_2 . All the catalytic tests were performed at a temperature of 100°C, a temperature at which all the blank tests showed no conversion of substrate. The Au@UiO-66- $NaBH_4$ was employed as catalyst (unless otherwise noted). During each test, aliquots were gradually taken out of the mixture, diluted with toluene and subsequently analyzed by GC-FID. All the fresh catalysts were activated under vacuum at 120°C for 3h prior to catalysis.

3. Characterization of the Au@UiO-66 materials

3.1 XRPD, nitrogen adsorption measurements and determination of the Au loading

The Au loading was determined of each Au@UiO-66 material by means of XRF (see Table 1). Approximately the same loading was obtained in each material, with an average of 0.1 mmol Au/g. Furthermore, the crystallinity of all the obtained Au@UiO-66 materials was verified by XRPD measurements (see Fig. S.1 Supporting Information). The XRPD pattern of each Au@MOF material presents the pure phase of the non-functionalized UiO-66. This explicitly shows that the framework integrity of the parent MOF was well preserved during the *in situ* synthesis of the Au NP. Additionally nitrogen sorption measurements were carried out to determine the Langmuir surface area of the Au@UiO-66 materials. The pristine UiO-66 material has a Langmuir surface area of approximately 1200 m²/g which corresponds to the reported value in literature¹³. After the *in situ* synthesis of the Au NP no significant changes are observed in the Langmuir surface area for the Au@MOF materials reduced by means of NaBH₄ and H₂. The Au@UiO-66-NaBH₄ and Au@UiO-66-H₂ material has a surface area of respectively 1172 m²/g and 1193 m²/g. In contrast, the material reduced by means of triethylamine, has a significant lower Langmuir surface area of 980 m²/g.

Table 1. Langmuir surface area and Au loading of the Au@UiO-66 materials.

Sample	Au loading (mmol/g)	S _{lang} (m ² g ⁻¹)
Au@UiO-66-NaBH ₄	0,12	1172
Au@UiO-66-triethylamine	0,09	980
Au@UiO-66-H ₂	0,1	1193

3.2 UV-Vis and XPS measurements

The formation of Au NP in the UiO-66 materials was further verified by means of UV-Vis diffuse reflectance spectroscopy measurements. In Fig 2. the UV-Vis spectra are depicted of the UiO-66 and the Au@UiO-66 materials. A broad peak centered at around 527 nm, characteristic for gold colloids, is observed in the Au@UiO-66 materials which is absent in the pristine material (Karen will elaborate more on the UV/VIS results)

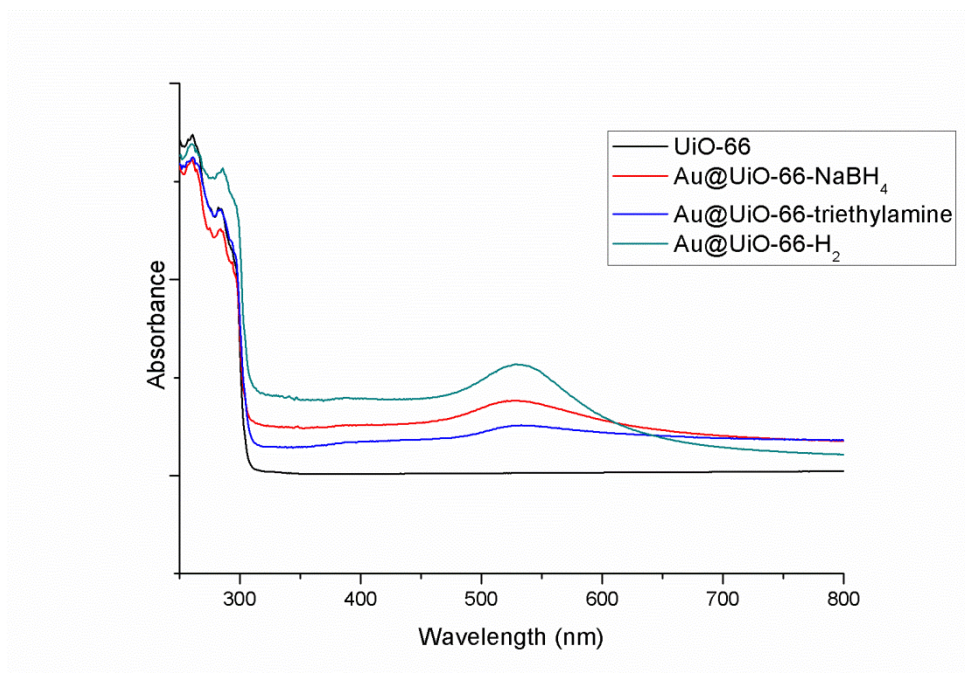


Fig.2 UV-Vis spectra of the pristine UiO-66 and Au@UiO-66 materials

To determine the valence state of the Au in the Au@UiO-66 materials X-ray photoelectron spectroscopy measurements were carried out. The XPS spectrum of Au@UiO-66-NaBH₄ displayed the Au 4f doublet (Au 4f_{7/2} at 83.9 eV and Au 4f_{5/2} at 87.5 eV) (Fig. 3). It can be deconvoluted in two pairs of doublets which can be ascribed to metallic Au and Au⁺¹ species at 83.8 and 85.1 eV (Au 4f_{7/2}) respectively. As can be seen from Fig. 3 the Au@UiO-66-NaBH₄ material possess a large amount of metal Au species and only a minority of Au⁺¹ is observed. The surface ratios of all the Au@UiO-66 materials are listed in Table 2. Although different reduction methods were examined, no significant differences are observed. As can be seen from this Table, each reduction method results in a similar amount of metallic Au species, approximately 88-95%, whereas only a small amount of Au⁺¹ is observed (5-12%).

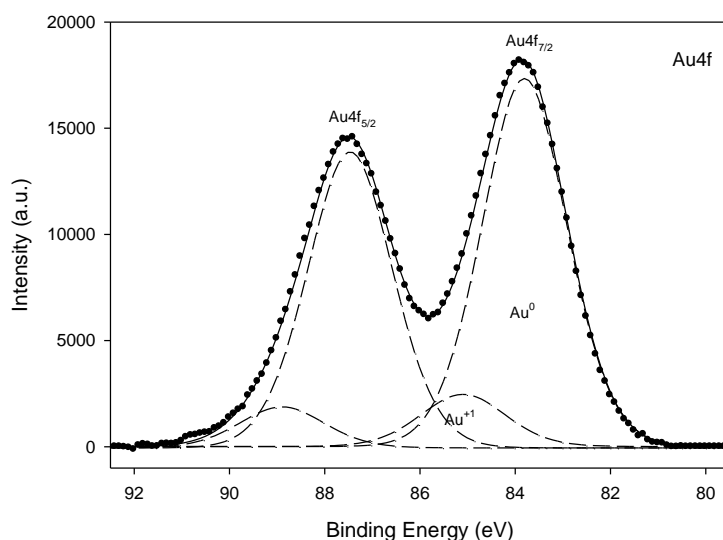


Figure 3. XPS spectrum in the Au 4f region of Au@UiO-66-NaBH₄

Table 2. Valence state of the Au NP in the Au@UiO-66 materials

Sample	Au(0)/%	Au(I)/%
Au@UiO66-NaBH ₄	87.7	12.3
Au@UiO66-triethylamine	95.3	4.7
Au@UiO66-H ₂	92.1	7.9

3.3 TEM measurements

4. Catalytic performance

In Table 3, an overview is presented of the examined substrates applying Au@UiO-66-NaBH₄ as catalyst. As can be seen from this Table, the catalyst exhibits a rather good conversion for the oxidation of benzyl alcohol and benzyl amine. For the substrate benzyl amine a conversion of 53 % was obtained after 24 hours of reaction with a selectivity of 100 % towards N-benzyl-1-phenylmethanimine whereas for benzyl alcohol 94 % of conversion was noted after 9 hours of catalysis with a selectivity of 100 % towards benzaldehyde. Furthermore, as can be seen from Table 3, the latter substrate can also be converted by air. By using 5 bar of air as oxidant 83 % of benzyl alcohol was converted after 23 hours of reaction with the same selectivity.

Table 3. Examined substrates using Au@UiO-66-NaBH₄ as catalyst.

Substrate	Oxidant	Conversion	Reaction time (hours)	Selectivity (%)
Benzyl alcohol	O ₂	94	9,5	100
Benzyl alcohol	air	83	23	100
Benzyl amine	O ₂	53	24	100

To study the influence of the size of the Au NP on the catalytic performance, Au@UiO-66-H₂, which has slightly smaller NP, was examined as a catalyst in the oxidation of benzyl alcohol and compared to the Au@UiO-66-NaBH₄. As previously mentioned, the latter material has Au NP in the range of 7±4 nm whereas the Au@UiO-66-H₂ has Au NP in the range of 5±3 nm. As can be seen from Fig 4, both catalyst show a similar conversion pattern. Approximately full conversion for both catalyst was obtained after 9 hours of catalysis demonstrating that the size of the Au NP has no significant influence on the catalytic performance. This is due to the fact that the catalytic mechanism for the Au@UiO-66 materials is different from the mechanism for Au@CeO₂. ...= correlation with the mechanistic results+*in situ* IR measurements....

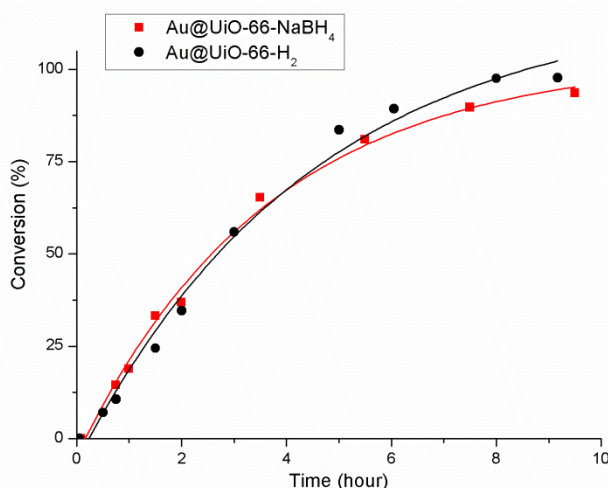


Figure 4. Benzyl alcohol conversion using Au@UiO-66-NaBH₄ and Au@UiO-66-H₂ as catalyst. Reaction conditions: substrate: benzyl alcohol, oxidant: O₂ solvent: toluene, temperature: 100°C

5. Reusability and stability tests

To examine the regenerability of the Au@UiO-66-NaBH₄, an additional run was performed. In Fig S.2, the first and second run is plotted using benzyl alcohol as substrate and in Table 4, the TON, TOF, selectivity and leaching percentage of each run is presented. As can be seen from Fig.S.2, a clear induction period is observed during the second run, which is probably due to the clogging of the pores. The latter observation was confirmed by nitrogen adsorption analysis (see Fig S.3). From Fig S.3 it can be seen that the pristine Au@UiO-66-NaBH₄ material has a surface area of 1172 m²/g whereas the material after catalysis only has a surface area of 865 m²/g. In the first run approximately full conversion of benzyl alcohol is observed after 9.5 hours of catalysis, whereas in the second run a conversion of 79 % is observed after 11 hours of reaction. The lower conversion in the second run is probably due to the loss of sample in the second run as the TON number in the first run is only slightly higher than the TON number obtained in the second run which are respectively 35 h⁻¹ and 28 h⁻¹. To demonstrate that the Au@UiO-66-NaBH₄ material could be reused for several times, a long run experiment was carried out using 2.5 mmol of benzyl alcohol instead of the original 0.25 mmol benzyl alcohol employed in the previous two run. The TON and TOF number for this long run are respectively 330 and 11.4 h⁻¹. Additionally the selectivity of the catalyst stays unaltered during these additional runs and only a small amount of Au NP was leached out. More specifically, 0.66 and 0.18 % of the Au species were leached out during the first two runs.

Table 4. TON, TOF, Selectivity and leaching percentage for each run using Au@UiO-66-NaBH₄ as catalyst

Run	TON	TOF (h ⁻¹)	Selectivity benzaldehyde (%)	Leaching Au (%)
Run 1	35 ^a	7,5 ^b	>99,9	0,66
Run 2	28 ^a	6 ^b	>99,9	0,18
Long run	330 ^c	11,4 ^d	>99,9	1,9

^aThe TON number was determined after 9,5 hours of catalysis, ^b the TOF number was determined after 1.5 hours of catalysis, ^c the TON number was determined after 118 hours of catalysis, ^d the TOF number was determined after 3 hours of catalysis.

Comparison of the XRPD pattern of the Au@UiO-66-NaBH₄ before catalysis and after each run, shows that the framework integrity of the MOF is preserved after the second run (Fig.5). Even after the long run the crystalline structure of the host material was preserved.

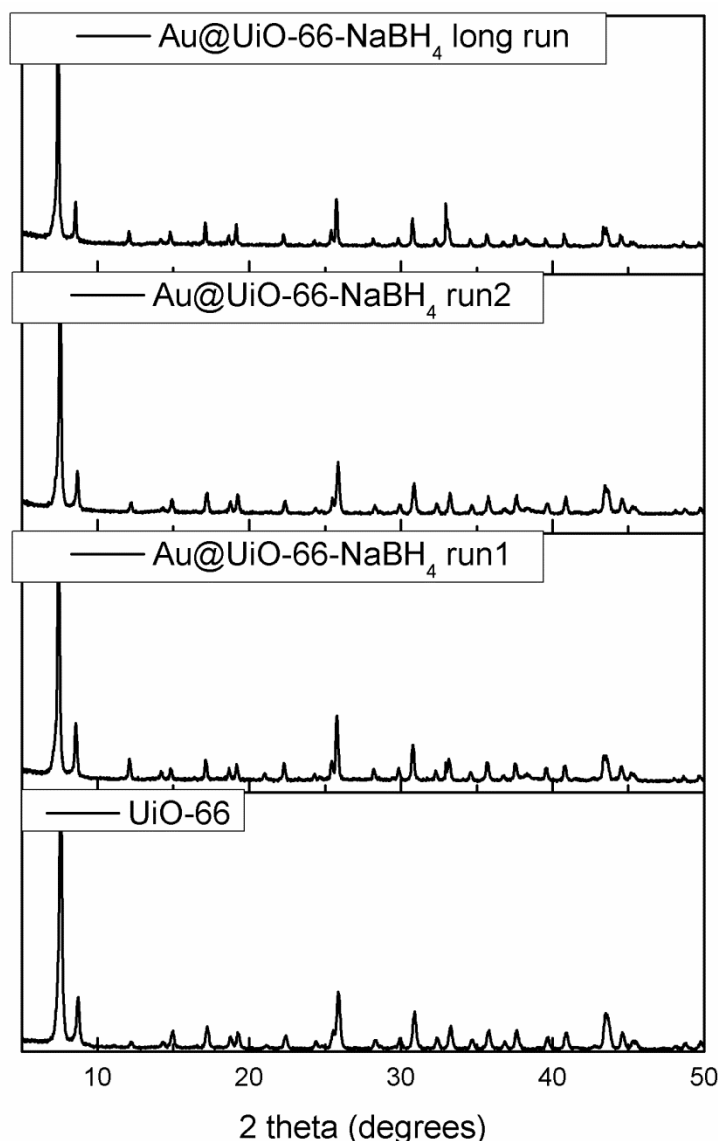


Figure 5. XRPD pattern of Au@UiO-66-NaBH₄ before catalysis and after catalytic test.

Additional proof for the stability of the Au@UiO-66-NaBH₄ was seen in the XPS and TEM measurements. The Au 4f spectrum of Au@UiO-66-NaBH₄ after catalysis showed two peaks at 83.9 and 87.5 eV assigned to Au 4f_{7/2} and Au 4f_{5/2}, respectively (Figure 6). After their deconvolution, an increase of the peak associated to Au⁺¹ is observed, therefore indicating a partial oxidation of the metallic Au to Au⁺¹ species during the catalytic test.

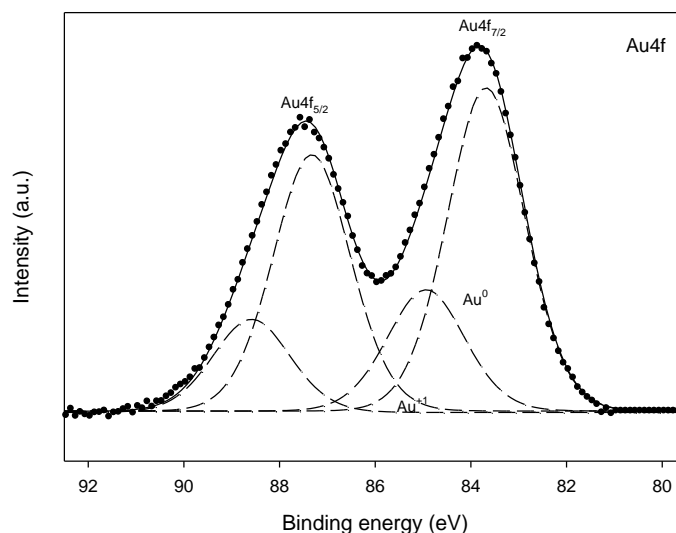


Figure 6. XPS spectra in the Au 4f region of Au@UiO-66-NaBH₄ after catalysis

6. Conclusions

Acknowledgements

K.L. acknowledge the financial support from the Ghent University BOF postdoctoral grant 01P06813T and UGent GOA Grant 01G00710.

References

- (a) Haruta, M.; Yamada, N.; Kobayashi, T.; Iijima, S., Gold Catalysts Prepared by Coprecipitation for Low-Temperature Oxidation of Hydrogen and of Carbon-Monoxide. *J Catal* **1989**, *115* (2), 301-309; (b) Della Pina, C.; Falletta, E.; Rossi, M., Update on selective oxidation using gold. *Chem Soc Rev* **2012**, *41* (1), 350-369.
- (a) Zhu, Y.; Qian, H. F.; Jin, R. C., An Atomic-Level Strategy for Unraveling Gold Nanocatalysis from the Perspective of Au-n(SR)(m) Nanoclusters. *Chem-Eur J* **2010**, *16* (37), 11455-11462; (b) Grirrane, A.; Corma, A.; Garcia, H., Highly active and selective gold catalysts for the aerobic oxidative condensation of benzylamines to imines and one-pot, two-step synthesis of secondary benzylamines. *J Catal* **2009**, *264* (2), 138-144; (c) Casanova, O.; Iborra, S.; Corma, A., Biomass into chemicals: One pot-base free oxidative esterification of 5-hydroxymethyl-2-furfural into 2,5-dimethylfuroate with gold on nanoparticulated ceria. *J Catal* **2009**, *265* (1), 109-116; (d) Mertens, P. G. N.; Corthals, S. L. F.; Ye, X.; Poelman, H.; Jacobs, P. A.; Sels, B. F.; Vankelecom, I. F. J.; De Vos, D. E., Selective alcohol oxidation to aldehydes and ketones over base-promoted gold-palladium clusters as recyclable quasihomogeneous and heterogeneous metal catalysts. *J Mol Catal a-Chem* **2009**, *313* (1-2), 14-21.

3. (a) Klitgaard, S. K.; DeLa Riva, A. T.; Helveg, S.; Werchmeister, R. M.; Christensen, C. H., Aerobic Oxidation of Alcohols over Gold Catalysts: Role of Acid and Base. *Catal Lett* **2008**, *126* (3-4), 213-217; (b) Mandal, S.; Bando, K. K.; Santra, C.; Maity, S.; James, O. O.; Mehta, D.; Chowdhury, B., Sm-CeO₂ supported gold nanoparticle catalyst for benzyl alcohol oxidation using molecular O₂. *Appl Catal a-Gen* **2013**, *452*, 94-104; (c) Wang, H.; Fan, W. B.; He, Y.; Wang, J. G.; Kondo, J. N.; Tatsumi, T., Selective oxidation of alcohols to aldehydes/ketones over copper oxide-supported gold catalysts. *J Catal* **2013**, *299*, 10-19; (d) Hallett-Tapley, G. L.; Silvero, M. J.; Bueno-Alejo, C. J.; Gonzalez-Bejar, M.; McTiernan, C. D.; Grenier, M.; Netto-Ferreira, J. C.; Scaiano, J. C., Supported Gold Nanoparticles as Efficient Catalysts in the Solvent less Plasmon Mediated Oxidation of sec-Phenethyl and Benzyl Alcohol. *J Phys Chem C* **2013**, *117* (23), 12279-12288; (e) Tanaka, A.; Hashimoto, K.; Kominami, H., Preparation of Au/CeO₂ Exhibiting Strong Surface Plasmon Resonance Effective for Selective or Chemoselective Oxidation of Alcohols to Aldehydes or Ketones in Aqueous Suspensions under Irradiation by Green Light. *J Am Chem Soc* **2012**, *134* (35), 14526-14533.
4. (a) Sekhar, A. C. S.; Sivaranjani, K.; Gopinath, C. S.; Vinod, C. P., A simple one pot synthesis of nano gold-mesoporous silica and its oxidation catalysis. *Catal Today* **2012**, *198* (1), 92-97; (b) Wang, X.; Chen, L. F.; Shang, M.; Lin, F.; Hu, J. C.; Richards, R. M., Nanoscale gold intercalated into mesoporous silica as a highly active and robust catalyst. *Nanotechnology* **2012**, *23* (29); (c) Ma, C. Y.; Dou, B. J.; Li, J. J.; Cheng, J.; Hu, Q.; Hao, Z. P.; Qiao, S. Z., Catalytic oxidation of benzyl alcohol on Au or Au-Pd nanoparticles confined in mesoporous silica. *Appl Catal B-Environ* **2009**, *92* (1-2), 202-208; (d) Zhu, K. K.; Hu, J. C.; Richards, R., Aerobic oxidation of cyclohexane by gold nanoparticles immobilized upon mesoporous silica. *Catal Lett* **2005**, *100* (3-4), 195-199; (e) Xie, X. Q.; Long, J. L.; Xu, J.; Chen, L. M.; Wang, Y.; Zhang, Z. Z.; Wang, X. X., Nitrogen-doped graphene stabilized gold nanoparticles for aerobic selective oxidation of benzylic alcohols. *Rsc Adv* **2012**, *2* (32), 12438-12446; (f) Yu, X. Q.; Huo, Y. J.; Yang, J.; Chang, S. J.; Ma, Y. S.; Huang, W. X., Reduced graphene oxide supported Au nanoparticles as an efficient catalyst for aerobic oxidation of benzyl alcohol. *Appl Surf Sci* **2013**, *280*, 450-455; (g) Wang, S.; Zhao, Q. F.; Wei, H. M.; Wang, J. Q.; Cho, M. Y.; Cho, H. S.; Terasaki, O.; Wan, Y., Aggregation-Free Gold Nanoparticles in Ordered Mesoporous Carbons: Toward Highly Active and Stable Heterogeneous Catalysts. *J Am Chem Soc* **2013**, *135* (32), 11849-11860.
5. (a) Leus, K.; Liu, Y. Y.; Van Der Voort, P., Metal-Organic Frameworks as Selective or Chiral Oxidation Catalysts. *Catal Rev* **2014**, *56* (1), 1-56; (b) Heine, J.; Muller-Buschbaum, K., Engineering metal-based luminescence in coordination polymers and metal-organic frameworks. *Chem Soc Rev* **2013**, *42* (24), 9232-9242; (c) Furukawa, H.; Cordova, K. E.; O'Keeffe, M.; Yaghi, O. M., The Chemistry and Applications of Metal-Organic Frameworks. *Science* **2013**, *341* (6149), 974-+.
6. Dhakshinamoorthy, A.; Garcia, H., Catalysis by metal nanoparticles embedded on metal-organic frameworks. *Chem Soc Rev* **2012**, *41* (15), 5262-5284.
7. Muller, M.; Turner, S.; Lebedev, O. I.; Wang, Y. M.; van Tendeloo, G.; Fischer, R. A., Au@MOF-5 and Au/MO_x@MOF-5 (M = Zn, Ti; x=1, 2): Preparation and Microstructural Characterisation. *Eur J Inorg Chem* **2011**, (12), 1876-1887.
8. Liu, H. L.; Liu, Y. L.; Li, Y. W.; Tang, Z. Y.; Jiang, H. F., Metal-Organic Framework Supported Gold Nanoparticles as a Highly Active Heterogeneous Catalyst for Aerobic Oxidation of Alcohols. *J Phys Chem C* **2010**, *114* (31), 13362-13369.
9. (a) Boronat, M.; Concepcion, P.; Corma, A.; Gonzalez, S.; Illas, F.; Serna, P., A molecular mechanism for the chemoselective hydrogenation of substituted nitroaromatics with nanoparticles of gold on TiO₂ catalysts: A cooperative effect

between gold and the support. *J Am Chem Soc* **2007**, *129* (51), 16230-16237; (b) Corma, A.; Garcia, H., Supported gold nanoparticles as catalysts for organic reactions. *Chem Soc Rev* **2008**, *37* (9), 2096-2126; (c) Abad, A.; Concepcion, P.; Corma, A.; Garcia, H., A collaborative effect between gold and a support induces the selective oxidation of alcohols. *Angew Chem Int Edit* **2005**, *44* (26), 4066-4069; (d) Abad, A.; Corma, A.; Garcia, H., Catalyst parameters determining activity and selectivity of supported gold nanoparticles for the aerobic oxidation of alcohols: The molecular reaction mechanism. *Chem-Eur J* **2008**, *14* (1), 212-222.

10. Ishida, T.; Nagaoka, M.; Akita, T.; Haruta, M., Deposition of Gold Clusters on Porous Coordination Polymers by Solid Grinding and Their Catalytic Activity in Aerobic Oxidation of Alcohols. *Chem-Eur J* **2008**, *14* (28), 8456-8460.

11. Esken, D.; Turner, S.; Lebedev, O. I.; Van Tendeloo, G.; Fischer, R. A., Au@ZIFs: Stabilization and Encapsulation of Cavity-Size Matching Gold Clusters inside Functionalized Zeolite Imidazolate Frameworks, ZIFs. *Chem Mater* **2010**, *22* (23), 6393-6401.

12. Zhu, J.; Wang, P. C.; Lu, M., Selective oxidation of benzyl alcohol under solvent-free condition with gold nanoparticles encapsulated in metal-organic framework. *Appl Catal a-Gen* **2014**, *477*, 125-131.

13. Biswas, S.; Van der Voort, P., A General Strategy for the Synthesis of Functionalised UiO-66 Frameworks: Characterisation, Stability and CO₂ Adsorption Properties. *Eur J Inorg Chem* **2013**, (12), 2154-2160.